

Infrared properties of $\text{La}_{2-x}(\text{Ca,Sr})_x\text{CaCu}_2\text{O}_{6+}$ single crystals

N. L. Wang,¹ P. Zheng,¹ T. Feng,¹ G. D. Gu,² C. C. Homes,² J. M. Tranquada,² B. D. Gaulin,³ and T. Timusk³

¹Institute of Physics, Chinese Academy of Sciences, P. O. Box 603, Beijing 100080, P. R. China

²Department of Physics, Brookhaven National Laboratory, P. O. Box 5000, Upton, NY 11973-5000, USA

³Department of Physics and Astronomy, McMaster University, Hamilton, Ontario L8S 4M1, Canada

(Dated: November 8, 2002)

The in-plane optical properties of two crystals of the bilayer cuprate $\text{La}_{2-x}(\text{Ca,Sr})_x\text{CaCu}_2\text{O}_{6+}$, one with excess Ca and $x = 0.10$ and the other with Sr and $x = 0.15$, were investigated over the frequency range of $45(25000 \text{ cm}^{-1})$. The optical conductivity has been derived from Kramers-Kronig transformation. Each crystal exhibits a peak at around 15000 cm^{-1} which corresponds to the charge-transfer gap of the parent insulator. With increasing carrier density, spectral weight shifts from the CT excitation to the low- ω region. For the superconducting sample ($x = 0.15$), the optical conductivity displays a peak in the far-infrared region, which shifts toward zero frequency with decreasing temperature. The temperature-dependent behavior favors a dynamical localization picture. A "pseudogap" feature is observed in the low-frequency reactance and the scattering rate spectra. Both the energy scale and the temperature dependence of the "pseudogap" are similar to other bilayer cuprates.

PACS numbers: 74.25.Gz, 74.72.-h

A common structural feature in all high- T_c cuprates is the presence of CuO_2 planes. High-temperature superconductivity depends not only on the carrier densities in the CuO_2 planes, but also on the number of CuO_2 planes in a unit cell (n). Within each family of cuprates, the superconducting transition temperature (T_c) increases with layer number for $n = 3$. This is well illustrated in Bi-, Tl-, and Hg-based systems. On the other hand, the transition temperatures for different families differ considerably. Among the most studied systems, the transition temperature T_c for bilayer materials $\text{YBa}_2\text{Cu}_3\text{O}_7$ and $\text{Bi}_2\text{Sr}_2\text{CaCu}_2\text{O}_{8+}$ at optimal doping exceeds 90 K, whereas the maximum T_c s for single-layer materials $\text{La}_{2-x}\text{Sr}_x\text{CuO}_{4+}$ and $\text{Bi}_2\text{Sr}_2\text{CuO}_{6+}$ are around 30–40 K. However, not all single-layer cuprates have such low transition temperatures. The maximum T_c for $\text{Tl}_2\text{Ba}_2\text{CuO}_6$ also reaches 90 K. For this reason, we classify $\text{La}_{2-x}\text{Sr}_x\text{CuO}_{4+}$ and $\text{Bi}_2\text{Sr}_2\text{CuO}_{6+}$ as low- T_c compounds within the high- T_c cuprates. At present, the reason for different T_c s in those materials is unclear.

Among all known bilayer materials, the La-based system $\text{La}_{1.9}\text{Ca}_{0.1}\text{Cu}_2\text{O}_{6+}$ (La2126) phase could be regarded as the simplest one.¹ The structure consists of a pair of pyramidal Cu-O layers facing one another, which are the only electronically active elements. Therefore, it is expected that this material could provide essential information about bilayer cuprates. Unfortunately, it has proven to be very difficult to make them superconducting. The reported superconducting transition temperatures for single crystals prepared under high oxygen pressure, or with Sr substitution for La, are below 50 K (Ref. 2). For polycrystalline samples, T_c can be a bit higher (around 60 K) than for the single crystals,¹ but it is not clear why higher T_c s are not observed. At present, La2126 must be considered as a low- T_c case among the bilayer high- T_c cuprates. It is of interest to investigate physical properties of this system and to compare them

with the single-layer $\text{La}_{2-x}\text{Sr}_x\text{CuO}_{4+}$ in the same family, as well as with other bilayer cuprates.

Owing to the difficulty of obtaining superconducting compounds, relatively few physical measurements have been made on this system. In this work we present the in-plane reactivity and optical conductivity data for single crystals of $\text{La}_{1.9}\text{Ca}_{0.1}\text{Cu}_2\text{O}_{6+}$ and $\text{La}_{1.85}\text{Sr}_{0.15}\text{CaCu}_2\text{O}_{6+}$. We shall show how optical spectra evolve with temperature for the more highly doped, slightly superconducting sample. To our knowledge, such temperature-dependent work has not been done previously. The only reported in-plane optical work³ was carried out at room temperature and for frequencies higher than 250 cm^{-1} .

Large single crystals of $\text{La}_{2-x}(\text{Ca,Sr})_x\text{CaCu}_2\text{O}_{6+}$ were grown by the traveling-solvent coating-zone technique. The Ca-doped $x = 0.10$ sample was grown in oxygen atmosphere at ambient pressure, while the Sr-doped $x = 0.15$ crystal was grown at an oxygen partial pressure of 10 bar. Based on the dopant concentration, and ignoring the uncertainty in the oxygen stoichiometry, the hole concentrations per CuO_2 plane are 0.05 and 0.075, respectively, spanning the threshold concentration for superconductivity in $\text{La}_{2-x}\text{Sr}_x\text{CuO}_{4+}$. Magnetization measurements with a superconducting quantum interference device indicate that the $x = 0.10$ sample is not superconducting down to the lowest measurement temperature 2 K, but that the Sr-substituted sample exhibits a weak superconducting response with an onset temperature of 28 K. For a given value of x , Kinoshita and Yamada⁴ found that both T_c and the Meissner signal increase with oxygen content (controlled by annealing in an oxygen atmosphere of increasing pressure). Our $x = 0.15$ crystal, grown in 10 bar O_2 , appears comparable to their sintered sample annealed in 50 atm (49 bar) O_2 .

The polarized reactance measurements from 45 to

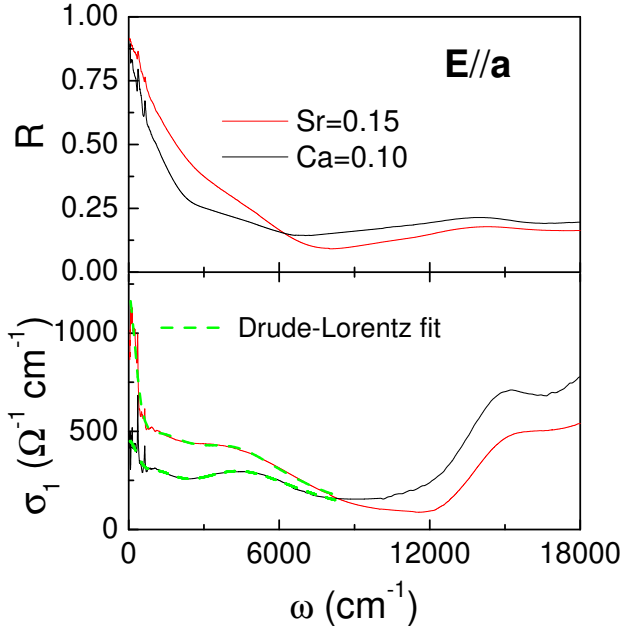


FIG. 1: The frequency dependent reflectance and conductivity of $\text{La}_{2-x}(\text{Ca,Sr})_x\text{CuO}_{6+x}$ with $x=0.10$ (Ca-doped) and $x=0.15$ (Sr-doped) at room temperature. The dash curves are Drude-Lorentz fits.

25000 cm^{-1} for E_{ka}-axis were carried out on a Bruker 66v/S spectrometer on polished surfaces of crystals, which were mounted on optically black cones in a cold-finger flow cryostat using an in situ overcoating technique.⁵ The optical conductivity spectra were derived from the Kramers-Kronig transformation. Since the high- ω extrapolation affects the conductivity spectra, especially the oscillator strength of the charge-transfer (CT) excitation, we connect the reflectance spectra to the high frequency data of $\text{La}_{2-x}\text{Sr}_x\text{CuO}_{4+x}$ by Uchida et al.⁶ The Hagen-Rubens relation was used for the low frequency extrapolation. It is found that different choices of dc conductivity values have minor effect on the conductivity in the measured frequency region.

Figure 1 shows the in-plane reflectance and optical conductivity spectra of the two crystals at room temperature. Below the reflectance edge at about 8000 cm^{-1} , the reflectance of the Ca-doped sample is substantially lower than that of the Sr-substituted sample, as one would anticipate based on the different nominal hole concentrations. In accord with this, the optical conductivity at low frequencies is considerably larger in the Sr-doped sample. Detailed analysis of the low- ω response will be presented in following paragraphs. At higher frequencies, the conductivity has two distinct absorption features: a Cu-O CT excitation near 15000 cm^{-1} and mid-infrared bands. With increasing carrier concentration, spectral weight is shifted from the CT excitation to the low- ω region. Comparisons with measurements on $\text{La}_{2-x}\text{Sr}_x\text{CuO}_{4+x}$ (Ref. 6), $\text{YBa}_2\text{Cu}_3\text{O}_{7-x}$ (Ref. 7), and Y-substituted $\text{Bi}_2\text{Sr}_2\text{CaCu}_2\text{O}_{8+x}$ (Ref. 8) indicate that the conductivity spectra are consistent with samples near

TABLE I: The parameters of the Drude-Lorentz fit to the room temperature data for the two samples. (All quantities are in units of cm^{-1} .)

Sample	ω_p	γ_D	ω_{11}	γ_{11}	ω_{p1}	ω_{21}	γ_{21}	ω_{p2}
Ca=0.10	4030	628	1400	2400	5100	4750	6000	9360
Sr=0.15	5575	433	1560	3140	8140	4600	5410	9230

the hole-concentration threshold for superconductivity.

The formation of a mid-infrared band is often seen in strongly correlated electronic materials. In doped Mott insulators, the mid-infrared peak is the first feature to appear at low doping; with increasing doping, weight grows at lower frequencies and eventually a Drude-like peak centered at $\omega = 0$ develops.⁹ This kind of evolution has been well documented in the single-layer $\text{La}_{2-x}\text{Sr}_x\text{CuO}_{4+x}$ cuprate.⁶ The observed change in bilayer $\text{La}_{1.9}\text{Ca}_{0.1}\text{Cu}_2\text{O}_{6+x}$ is consistent with the general feature. The accumulation of low- ω spectral weight could be quantitatively analyzed from the partial sum rule, $N_{\text{eff}}(\omega) = (2m_e V / e^2) \int_0^\omega \sigma_1(\omega') d\omega'$, where m_e is the bare electron mass and V is the volume of the unit cell. Usually, an integral of the spectral weight below the frequency of reflectance or conductivity minimum would give approximately the overall plasma frequency. However, since the $\epsilon_1(\omega)$ contains obviously different components, such integration may overcount the contributions of free carriers. A Drude-Lorentz analysis would be more appropriate in this case. The general formula for the optical conductivity of the Drude-Lorentz model is¹⁰

$$\epsilon_1(\omega) = \frac{\omega_p^2}{4} \frac{\gamma_D}{\omega^2 + \frac{\gamma_D^2}{4}} + \sum_j \frac{\omega_{pj}^2}{4} \frac{\gamma_j \omega^2}{(\omega_j^2 - \omega^2)^2 + \frac{\gamma_j^2 \omega^2}{4}} \quad (1)$$

where ω_p and γ_D in the Drude term are the plasma frequency and the relaxation rate of the free charge carriers, while ω_j , γ_j , and ω_{pj} are the resonance frequency, the damping, and the mode strength of the Lorentz oscillators, respectively. As shown in Fig. 1, the main features in $\epsilon_1(\omega)$ below the frequency of the reflectance minimum can be well reproduced by the combination of one Drude component and two Lorentz oscillators. The fitting parameters in the Drude-Lorentz model for the two samples are shown in Table I. The overall evolution of optical spectra with doping is similar to other high- T_c cuprates. In the following we shall mainly focus on the temperature-dependent behavior of the superconducting sample in the low-energy region.

Figure 2 shows the reflectance and conductivity spectra below 2000 cm^{-1} at different temperatures for the Sr=0.15 sample. In general, the temperature dependence of the optical spectra shows a metallic response, with the low- ω conductivity becoming significantly enhanced with decreasing temperature. At the same time, $\epsilon_1(\omega)$ at 200 K and 300 K exhibits a peak at finite frequency, reaching 150 cm^{-1} at 300 K, in contrast to the $\omega = 0$ peak expected for standard Drude behavior.

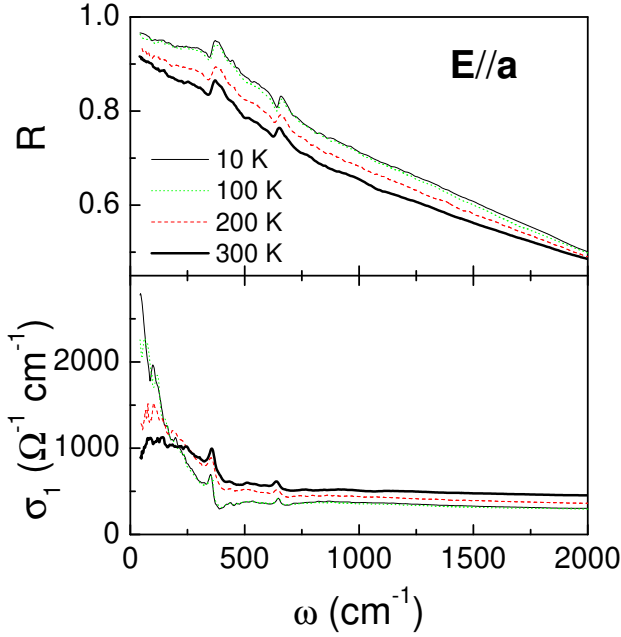


FIG. 2: The frequency dependent reflectance and conductivity of $\text{La}_{1.85}\text{Sr}_{0.15}\text{CaCu}_2\text{O}_{6+}$ at different temperatures.

A peak at finite frequency has been observed in a number of high- T_c cuprates^{11,12,13,14,15,16} as well as in many other correlated materials.^{17,18} Several possibilities have been suggested for the origin of the peak. The simplest one is that it is related to carrier localization caused by disorder, defects, or impurities, i.e. Anderson localization.^{12,13,14} This interpretation received support from several studies where a finite-frequency peak appeared when defects or impurities were deliberately introduced into samples.^{13,14,19} For example, for the pure $\text{YBa}_2\text{Cu}_3\text{O}_{7-x}$ at optimal doping, there is no such peak at finite energy; however, when some impurities such as Zn were introduced into the sample, or when the sample was irradiated by high-energy ions, the peak appeared at $\omega \neq 0$. This picture cannot explain those cases where there are no apparent defects or impurities¹⁸; furthermore, for Anderson-type localization the effect should become more significant at low temperature, while in many experiments, including the present study, the peak was observed only at high temperatures. Nevertheless, the comparison to systems with defects is relevant in our case, as diffraction studies of $\text{La}_{2-x}(\text{Ca,Sr})_x\text{CuO}_{4+}$ have found a tendency for 5 to 15% of the Ca sites, located between the CuO_2 bilayers, to be replaced by La.^{20,21,22,23}

A finite-energy peak has also been observed in systems with static charge stripes, such as Nd-doped $\text{La}_{2-x}\text{Sr}_x\text{CuO}_{4+}$ (Refs. 24,25) and in Nd-free $\text{La}_{2-x}\text{Sr}_x\text{CuO}_{4+}$ in which one might expect the existence of dynamical stripe fluctuations.^{26,27} Recent neutron scattering measurements on $\text{La}_{2-x}(\text{Ca,Sr})_x\text{CuO}_{6+}$ have found no evidence of any charge ordering.^{23,28} At the same time, elas-

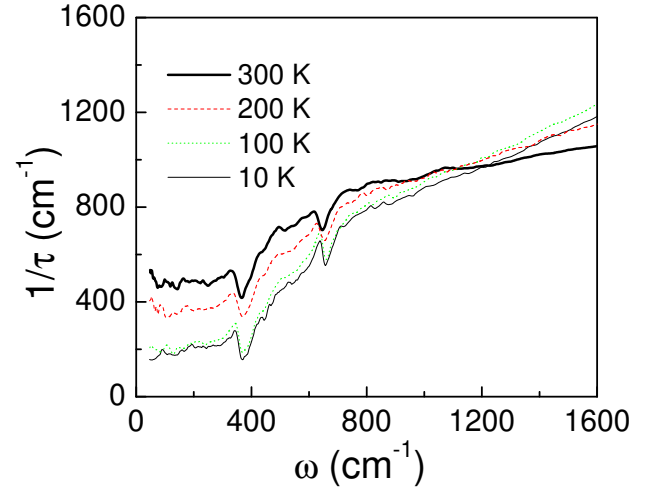


FIG. 3: The frequency-dependent scattering rate of $\text{La}_{1.85}\text{Sr}_{0.15}\text{CaCu}_2\text{O}_{6+}$ at different temperatures.

tic scattering from antiferromagnetic clusters has been observed,^{23,28} clearly indicating some form of inhomogeneity.

Recently, Takenaka et al.^{16,17} have studied the finite-energy-peak phenomenon in $\text{La}_{2-x}\text{Sr}_x\text{CuO}_{4+}$ and $\text{La}_{1-x}\text{Sr}_x\text{MnO}_3$. They linked its occurrence to the condition that the resistivity at high temperature exceeds the Mott criterion ρ_{Mott} , which corresponds to the point at which the quasiparticle mean free path ℓ becomes comparable to the Fermi wavelength $\lambda_F = 2\pi/k_F$ (Refs. 29,30). Distinct from the low- T Anderson localization caused by elastic scattering due to disorder or impurities, the high- T phenomenon is called "dynamic" localization, and is attributed to strong inelastic scattering. Our present results appear to correspond to the latter case.

It is interesting to compare $\text{La}_{1.85}\text{Sr}_{0.15}\text{CaCu}_2\text{O}_{6+}$ with other heavily underdoped cuprates. One way in which such comparisons are often made is to plot the scattering rate vs. frequency, obtained by applying the extended Drude model to the optical conductivity.³¹ In optimally-doped cuprates, the scattering rate is linear in both frequency and temperature above T_c and develops a "gap-like" suppression below T_c . In underdoped samples, the scattering rate depression sets in well above transition temperature. The depression of the scattering rate at $T > T_c$ has frequently been associated with pseudogap phenomena³¹; however, it should be noted that no depression of the low-energy effective density of in-plane charge carriers has been clearly demonstrated in the pseudogap regime of any cuprates, contrary to the situation for charge motion along the c -axis.³²

Figure 3 shows the scattering rate spectra at different temperatures for the $\text{La}_{1.85}\text{Sr}_{0.15}\text{CaCu}_2\text{O}_{6+}$ sample being obtained from the extended Drude model using the plasma frequency of 5575 cm^{-1} . We can see that the scattering rate deviates from the linear- ω dependence below 700 cm^{-1} even at room temperature, an energy scale very similar to that found in other under-

doped cuprates.³¹ There is a substantial residual scattering of about 480 cm^{-1} at low frequencies which is in good agreement with the 433 cm^{-1} width of the low- ω peak in $\chi''(\omega)$. At lower temperatures, the residual scattering decreases. In accord with this, we find the narrowing of the low- ω peak in $\chi''(\omega)$. In the raw data of the reactance, the "gap-like" feature of the relaxation rate appears as the shoulder-like structure, which can also be seen clearly in Fig. 2.

Finally, we make some comments about the superconducting condensate. The difference between the reactance at low temperature and that at T_c in low frequencies (within the gap energy) could be taken as a rough measure of the superconducting condensate density.³³ From the reactance below and above the superconducting transition temperature, no obvious difference could be detected, indicating that the condensed carrier density is very small in this sample. Within current understanding, the superconducting gap reflects the pairing strength, while the condensed carrier density is an indication of the phase stiffness of the pairing.^{34,35,36} Our result suggests that the strength of pairing coherence is quite weak. This can only partially be ascribed to the relatively low carrier density doped into the material. The low superconducting condensate is qualitatively

consistent with the low T_c of the material.

In summary, we have determined the in-plane optical properties of two $\text{La}_{2-x}(\text{Ca,Sr})_x\text{CuO}_{6+y}$ crystals. Both exhibit a peak at around 15000 cm^{-1} which corresponds to the charge-transfer gap of the parent insulator. With increasing carrier density, spectral weight shifts from the CT excitation to the low- ω region. For the superconducting sample, the optical conductivity displays a peak in the far-infrared region that shifts towards zero frequency with decreasing temperature. The feature is similar to underdoped $\text{La}_{2-x}\text{Sr}_x\text{CuO}_{4+y}$, suggesting some dynamical localization. The low-frequency reactance has some knee structure between 400 – 700 cm^{-1} , apparent at all measured temperatures; similar features in other cuprates have been interpreted as evidence of a pseudogap state. Furthermore, the superfluid density is very low, consistent with the low T_c , suggesting that the strength of pairing coherence is quite weak.

This work was in part supported by National Science Foundation of China (No.10025418). The work at Brookhaven National Laboratory was supported by the U.S. Department of Energy under contract DE-AC02-98CH10886.

Electronic address: nlwang@aphy.iphy.ac.cn

- ¹ R. J. Cava, B. Batlogg, R. B. van Dover, J. J. Krajewski, J. V. W. Aszczak, R. F. Fleming, W. F. Peck Jr., L. W. Rupp Jr., P. Marsh, A. C. Woodward, J. M. Jamieson, and L. F. Schneemeyer, *Nature (London)* **345**, 602 (1990).
- ² T. Watanabe, K. K. Inoshita, and A. Matsuda, *Phys. Rev. B* **47**, 11544 (1993).
- ³ H. Shibata, T. Watanabe, K. K. Inoshita, A. Matsuda, and T. Yamada, *Phys. Rev. B* **48**, 14027 (1993).
- ⁴ K. K. Inoshita and T. Yamada, *Phys. Rev. B* **46**, 9116 (1992).
- ⁵ C. C. Homes, M. Reedyk, D. A. Crandles, and T. Timusk, *Appl. Opt.* **32**, 2973 (1993).
- ⁶ S. Uchida, T. Ido, H. Takagi, T. Arima, Y. Tokura, and S. Tajima, *Phys. Rev. B* **43**, 7942 (1991).
- ⁷ S. L. Cooper, D. Reznik, A. Kotz, M. A. Karlow, R. Liu, M. V. Klein, W. C. Lee, J. G. Papantzas, D. M. Ginsberg, B. W. Veal, and A. P. Paulikas, *Phys. Rev. B* **47**, 8233 (1993).
- ⁸ N. L. Wang, A. W. McConnell, and B. P. Clayman, *Phys. Rev. B* **60**, 14883 (1999).
- ⁹ Y. Okimoto and Y. Tokura, *J. of Supercond.* **13**, 271 (2000).
- ¹⁰ T. Timusk and D. Tanner, in *Physical Properties of High Temperature Superconductors I*, edited by D. M. Ginsberg (World Scientific, Singapore, 1989).
- ¹¹ A. A. Tsvetkov, J. Schutzmann, J. I. Gorina, G. A. Kalashnikova, and D. van der Marel, *Phys. Rev. B* **55**, 14152 (1997).
- ¹² T. Timusk, D. N. Basov, C. C. Homes, A. V. Puchkov, and M. Reedyk, *J. Supercond.* **8**, 437 (1995).
- ¹³ D. N. Basov, A. V. Puchkov, R. A. Hughes, T. Strach, J. Preston, T. Timusk, D. A. Bonn, R. Liang, and W. N. Hardy, *Phys. Rev. B* **49**, 12165 (1994).
- ¹⁴ D. N. Basov, B. Dabrowski, and T. Timusk, *Phys. Rev. Lett.* **81**, 2132 (1998).
- ¹⁵ J. J. McGuire, M. W. Indt, T. Startsev, T. Timusk, D. Colson, and V. Viallet-Guillen, *Phys. Rev. B* **62**, 8711 (2000).
- ¹⁶ K. Takenaka, R. Shiozaki, S. Okuyama, J. Nohara, A. Ohsuka, Y. Takayanagi, and S. Sugai, *Phys. Rev. B* **65**, 092405 (2002).
- ¹⁷ K. Takenaka, R. Shiozaki, and S. Sugai, *Phys. Rev. B* **65**, 184436 (2002).
- ¹⁸ P. Kostic, Y. Okada, N. C. Collins, Z. Schlesinger, J. W. Reiner, L. Klein, A. Kapitulnik, T. H. Geballe, and M. R. Beasley, *Phys. Rev. Lett.* **81**, 2498 (1998).
- ¹⁹ N. L. Wang, S. Tajima, A. I. Rykov, and K. Tomimoto, *Phys. Rev. B* **57**, R11081 (1998).
- ²⁰ F. Izumi, E. Takayama-Muromachi, Y. Nakai, and H. Amano, *Physica C* **157**, 89 (1989).
- ²¹ T. Sakurai, T. Yamashita, J. O. Willis, H. Yamachi, S. Tanaka, and G. H. Kwei, *Physica C* **174**, 187 (1991).
- ²² K. K. Inoshita, F. Izumi, T. Yamada, and H. Amano, *Phys. Rev. B* **45**, 5558 (1992).
- ²³ C. Ulrich, S. Kondo, M. Reehuis, H. He, C. Bernhard, C. Niedermayer, F. Bouree, P. Bourges, M. Ohl, H. M. Ronnow, H. Takagi, and B. Keimer, *Phys. Rev. B* **65**, 220507(R) (2002).
- ²⁴ S. Tajima, N. L. Wang, N. Ichikawa, H. Eisaki, S. Uchida, H. Kitanaka, T. Hanaguri, and A. M. Aeda, *Europhys. Lett.* **47**, 715 (1999).
- ²⁵ M. Dumm, D. N. Basov, S. Komiyama, Y. Abe, and Y. Ando, *Phys. Rev. Lett.* **88**, 147003 (2002).
- ²⁶ F. Venturini, Q. M. Zhang, R. Hackl, A. Lucarelli, S. Lupi,

- M. Ohtolani, P. Calvani, N. Kikugawa, and T. Fujita, *Phys. Rev. B* **66**, 060502(R) (2002).
- ²⁷ A. Lucarelli, S. Lupi, M. Ohtolani, P. Calvani, P. Maselli, M. Capizzi, P. Giura, H. Eisaki, N. Kikugawa, T. Fujita, M. Fujita, and K. Yamada, *preprint*.
- ²⁸ M. Hcker, Y. J. Kim, J. M. Tranquada, G. D. Gu, and J. W. Lynn, *unpublished*.
- ²⁹ N. F. Mott, *Metal-Insulator transitions*, 2nd ed. (Taylor and Francis, London, 1990).
- ³⁰ V. J. Emery and S. A. Kivelson, *Phys. Rev. Lett.* **74**, 3253 (1995).
- ³¹ A. V. Puchkov, D. N. Basov, and T. Timusk, *J. Phys.: Condens. Matter* **8**, 10049 (1996).
- ³² C. C. Homes, T. Timusk, R. Liang, D. A. Bonn, and W. N. Hardy, *Phys. Rev. Lett.* **71**, 1645 (1993).
- ³³ T. Timusk and C. C. Homes, *cond-mat/0209371*.
- ³⁴ Y. J. Uemura, G. M. Luke, B. J. Stemlieb, J. H. Brewer, J. F. Carolan, W. N. Hardy, R. Kadono, J. R. Kempton, R. F. Kie, S. R. Kretzmann, P. Mulhem, T. M. Riseman, D. L. Williams, B. X. Yang, S. Uchida, H. Takagi, J. Gopalakrishnan, A. W. Sleight, M. A. Subramanian, C. L. Chien, M. Z. Cieplak, Gang Xiao, V. Y. Lee, B. W. Statt, C. E. Stronach, W. J. Kossler, and X. H. Yu, *Phys. Rev. Lett.* **62**, 2317 (1989).
- ³⁵ V. J. Emery and S. A. Kivelson, *Nature* **374**, 434 (1995).
- ³⁶ D. L. Feng, A. Damascelli, K. M. Shen, N. Motoyama, D. H. Lu, H. Eisaki, K. Shimizu, J.-I. Shimoyama, K. Kishio, N. Kaneko, M. Greven, G. D. Gu, X. J. Zhou, C. Kim, F. Ronning, N. P. Armitage, and Z. X. Shen, *Phys. Rev. Lett.* **88**, 107001 (2002).